CODEN [USA]: IAJPBB ISSN: 2349-7750

INDO AMERICAN JOURNAL OF
PHARMACEUTICAL SCIENCES

http://doi.org/10.5281/zenodo.1482790

Available online at: http://www.iajps.com Research Article

BIOACTIVITY OF GREEN SYNTHESIZED SILVER NANOPARTICLES FROM *CALOTROPIS GIGANTEA (L.) R.BR* LEAVES AND STEMS

Vijaya Subhashini. M[1]and Dinakaran .S[1]*

[1] Department of Zoology, The Madura College, Madurai-625011

Abstract:

In this study, we have synthesised and analysed the potential efficiency of the green synthesized silver nanoparticles (AgNPs) using Calotropis gigantea (Linn) R. Br leaves and stems extract as a reducing and stabilizing agent under surfactant-free conditions. The formation of AgNPs is monitored by recording the UV–vis absorption spectra. The green synthesized AgNPs were characterized by UV–visible, FT-IR, XRD, EDAX, and SEM techniques. The green synthesized AgNPs of C. gigantea (Linn) R. Br leaves and stems were significantly showed more effective free radical scavenging activity. Synthesised silver nanoparticles shows potent antibacterial, antifungal, antibiofilm, antiangiogenic, mosquitocidal activity. Also the green synthesized silver nanoparticles exhibit cytotoxicity against Hep2 and AGS cell lines, further it may use effectively in treatment of carcinomas. The results observed in the present study showed the promising potential of C. gigantea (Linn.) R.Br- synthesised AgNPs for the development of novel antimicrobials, antibiofilm, and antiangiogenesis, mosquitocidal, anticancer and for various purposes.

Keywords: *Green synthesizes AgNPs, UV–visible, FT-IR, XRD, EDX, and SEM.*

***Corresponding Author:**

Dinakaran .S,

Head, Department of Zoology,
The Madura College, Madurai-625011,
Tamilnadu, India.
Tel: +919994900064,
dinkarji@gmail.com.

QR code

Please cite this article in press Vijaya Subhashini and Dinakaran .S, ***Bioactivity of Green Synthesized Silver Nanoparticles From Calotropis Gigantea (l.) R.br Leaves and Stems.,*** *Indo Am. J. P. Sci, 2018; 05(11).*

INTRODUCTION:

Nanoscience is the study of phenomena and manipulation of materials at atomic molecular and macromolecular scales. Now this field of science and technology, living organisms show huge potentiality for various applications. Nanotechnology deals with the design, production, characterization & application of nanoscale, devices and systems by controlling shape and size at the nano scale. It involves the production, manipulation and use of materials ranging in size from less than a micron to that of individual atoms from not only chemical approaches but also biological materials. Silver nanoparticles synthesized which are quite stable and no visible changes are observed even after a month or so, if the nanoparticle solutions are kept in light proof condition. As nanoparticles have great application in medical world like gene therapy, cancer therapy, drug delivery etc. So medical world also easily accept the plant world for nanoparticle synthesis and welcome the angiosperms for their potentiality of synthesis of non-polluted, environmentally acceptable, safety for human health nanoparticles (1).

Nanotechnology is an emerging field with large range of applications in areas such as cosmetics, health care, environmental health, optics, mechanics, biomedical sciences, chemical industries, space industries, electronics, drug-gene delivery etc., Green synthesis methods make use of to some extent pollutant-free chemicals for prepare of nanostructures. It embraces the use of ecofriendly & secure solvents such as water, natural extracts. So biological approaches using microorganisms & plants or plant extracts for prepare of metal nanoparticles have been recommended as safe options to chemical methods. The 'green' environment friendly processes in chemistry and chemical technologies are becoming increasingly popular and are much needed as a result of worldwide problems associated with environmental concerns (2-5). Silver is the one of the most commercialized nanomaterial for a wider range of application. In the present work, we have synthesized silver nanoparticles phytosynthesis and ecofriendly method and the resulting sample were characterized by FTIR, UV, XRD, EDX and SEM and then analyzed for the various applications.

Study area:

Azhagar hills of Eastern Ghats is lying approximately between 77°30 and 78°20 longitude and 10°05' – 10°09' latitude. The elevation of the area of investigation ranges from 650 to 3000 feet above sea level. Variations in the altitude and rainfall have a bearing on the vegetation in general. The floristic divisions of the area of investigation consist of deciduous thorny scrub forest, dry deciduous forest, and evergreen moist mixed deciduous forest and savannah grasslands.

Botanical name: ***Calotropis gigantea (L.) R.Br***

Taxonomic classification:

Kingdom: Plantae – Plants

Phylum: Tracheophyta– Vascular plants

Subphylum: Euphyllophytina– Seed plants

Class: Magnoliopsida – Flowering plants

Subclass: Asteridae – Dicotyledons

Order: Gentianales

Family: Apocynaceae – Milkweed family

Subfamily: Asclepiadoideae

Genus: Calotropis – calotropis

Species: gigantea (L.) R.Br

Plate:1 ***Calotropis gigantea (Linn) R. Br*** **Plant**

Plate 1 ***Calotropis gigantea (Linn) R. Br*** **Plant, Taxonomic classification and photograph of** ***Calotropis gigantea (Linn) R. Br*** **(white flowers).**

Distribution: Throughout India, Ceylon-Malay Island, and S. China. (6)

Botanical Description:
A tall shrub reaching 2.4-3m high; yellowish white, furrowed; branches stout, terete, more or less covered (especially the younger ones) with fine appressed cottony pubescence. Leaves 1-20 by 3.8-10 cm, sessile or nearly so, elliptic-oblong or abovate-oblong, acute, thick, glaucous-green, clothed beneath and more or less above with fine cottony tomenum; base narrow, cordate. Flowers in odourous, purplish or white. Calyx divided to the base; sepals 6 by 4 mm, ovate, acute, cottony. Corolla 2cm long or more; lobes 1.3-1.6cm long, deltoid-ovate, subacute, revolute and twisted in age; lobes of the corona1.3cm. Long by 5mm. pubescent on the slightly thickened margin, the apex rounded with 2 obtuse auricles just below it. Follicles 9-10 cm. Long, broad, thick, fleshy, ventricose, green. Seeds numerous, 6 by 5 mm. broadly ovate, flattened narrowly margined, minutely tomentose, brown coma 2.5-3.2 cm long.

MATERIALS AND METHODOLOGY:

CHEMICALS
Silver nitrate ($AgNo_3$) analytical grade was purchased from sigma Aldrich chemical Pvt. Ltd, distilled water, trypan blue dye.All the chemicals and solvents used were of the highest purity and analytical grade.

Collection of plant material:
Calotropis gigantea (white flower) plant parts were collected from different locations of Azhagar Hill (Eastern Ghats), Madurai, Tamilnadu, South India during the year 2015–2016. Plant specimens were photographed and collected on the spot (Azhagar Hill area), pressed, dried (in herbarium sheet) authenticated by Dr. S. John Britto S.R in Rapinat Herbarium as "MVS OO14 *Calotropis gigantea (Linn) R. Br".*

Preliminary phytochemical screening
Preliminary phytochemical analysis was performed for establishing the phyto-constituents (alkaloids, tannins, glycosides, steroids and terpenoids) present in the leaf and stem extracts. Chemical tests for the screening and identification of bioactive chemical constituents in the medicinal plants under study were carried out in extracts using the standard procedures as described by Sofowara (1993), Trease and Evans (1989), (2002) and Harborne (1973). Identification tests for the various chemicals were carried out to test the presence of various chemical constituents.

Phytochemical analysis:
Methods of Qualitative phytochemical analysis
The leaf and stem extracts were tested for the presence of bioactive compounds by using following standard methods (7-9).

Preparation of *Calotropis gigantea (Linn) R. Br* leaves and stems extracts (Garima Singha *et al.*, 2011).
The leaves and stems were separately washed thrice with distilled water to avoid fine dust particles on its surface. Following thorough washing, the leaves and stems were completely air dried for about 15 minutes to remove residual moisture. About 20 grams of finely chopped leaves were boiled with 100 ml of distilled water for 30 minutes at 60°C. After cooling, the leaf and stem extract is obtained as a clear filtrate using Whatmann No: 1 filter paper individually and it was used for further analysis.

Optimization of silver nanoparticle synthesis (Veerasamy *et al*., 2011).
Optimized silver nanoparticles synthesis was obtained by variation and fixation of different parameters such as temperature, time, ratio of plant extract to silver nitrate solution, concentration of silver nitrate solution and pH in order to achieve maximum yield.

Temperature
About 5 ml of *C. gigantea (Linn) R. Br* leaves and stems extracts were added to 45 mL of 1 mM $AgNO_3$ solution was used for optimization of temperature, where the reaction temperature was maintained at 30, 60, 90 and 120 C^0 respectively, using water bath. The absorbance of the resulting solutions was measured spectrophotometrically**.**

Time
About 5 ml of *C. gigantea (Linn) R. Br* leaves and stems extracts were added to 45 mL of 1 mM $AgNO_3$ solution was used to optimize the time required for the completion of reaction, where the reaction was monitored from the start of the reaction to 6, 12, 18, 24hours time period. The reaction mixture was also monitored after 24 hours incubation time. The absorbance of the resulting solutions was measured spectrophotometrically**.**

Ratio
Various 1:5, 1:6, 1:7, 1:8, 1:9 ratios of *C. gigantea (Linn) R. Br* leaves and stems extracts: silver nitrate solution were added individually to optimize the ratio of leaves extracts and stems extracts separately to silver nitrate solution. The absorbance of the resulting

solutions was measured spectrophotometrically.

Concentration

About 5 ml of *C. gigantea (Linn) R. Br* leaves and stems extracts were added to 45 mL of 0.5 mM, 1 mM, 1.5 mM, 2 mM $AgNO_3$ solution was used to optimize the concentration of silver nitrate solution. The absorbance of the resulting solutions was measured spectrophotometrically.

pH

About 5 ml of *C. gigantea (Linn) R. Br* leaves and stems extracts were added to 45 mL of 1 mM $AgNO_3$ solution was used for optimization of pH where the reaction pH was maintained at 5, 7, 8 and 9 respectively. The pH was adjusted by using 0.1 N HCl and 0.1N NaOH. The absorbance of the resulting solutions was measured spectrophotometrically.

Characterization of silver nanoparticles

The *Calotropis gigantea (Linn.) R.Br* leaves and stems extract silver synthesized nanoparticles were characterized by using various spectral analysis.

UV-visible absorbance spectroscopy (Shankar *et al.*, 2004)

UV-Visible spectroscopy analysis was carried out on a Systronic UV-Visible absorption spectrophotometer 117 with a resolution of ±1nm between 200-1000nm processing a scanning speed of 200nm/min. Equal amounts of the suspension (0.5ml) was taken and analyzed at room temperature. The progress of the reaction between metal ions and the leaf extract were monitored by UV-Visible spectra of silver nanoparticles in aqueous solution with different wavelength in nanometers from 340 to 600nm. The reduction of silver ions and formation of silver nanoparticles occurred within an hour of reaction .Control was maintained by using $AgNO_3$.

Fourier transform infrared spectroscopy (FTIR) (Manopriya *et al.*, 2011)

For FTIR measurements, Perkin Elimer-spectrum RXI model was used. The synthesized silver nanoparticles solution was centrifuged at 10000 rpm for 30 minutes. The pellet was washed thrice with 5 ml of deionized water to get rid of the free proteins or enzymes that are not capping the silver nanoparticles. The pellet was dried by using vacuum drier. Fourier transformed infrared spectra is generated by the absorption of electromagnetic radiation within the frequency range 400 to 4000 $cm^{-1.}$

Scanning electron microscopy (SEM) (Savithramma *et al.*, 2011)

The pellet was subjected for SEM analysis. Thin films of the sample were prepared on a carbon coated copper grid by just dropping a very small amount of the sample on the grid, extra solution was removed using a blotting paper and then the film on the SEM grid were allowed to dry for analysis.

X-ray diffraction (XRD) (Prema *et al*, 2010)

A thin film of the silver nanoparticle was made by dipping a glass plate in a solution and carried out for X-ray diffraction studies. The crystalline silver nanoparticle was calculated from the width of the XRD peaks and the average size of the nanoparticles can be estimated using the Debye–Scherrer equation (Rau, 1962): $\mathbf{D= k\lambda / \beta cos\theta}$

Where D = Thickness of the nanocrystal, k = Constant, λ = Wavelength of X-rays, β = Width at half maxima of (111) reflection at Bragg's angle 2θ, θ = Bragg angle. The size of the silver nanoparticle was made from the line broadening of the (111) reflection using the Debye-Scherrer formula. According to the formula, Constant (K) = 0.94, Wave length (λ) = 1.5406×10^{-10}

Energy dispersive X-ray analysis (Mahendran Vanaja et al., 2013)

Energy dispersive analysis X-ray (EDX) analysis takes advantage of the photon nature of the light. In the X-ray range the energy of a single photon is just sufficient to produce a measurable pulse X-ray. A semiconductor material is used to detect the X-ray along with processing electronics to analysis the spectrum.

***In vitro* antioxidant assays**

Estimation of total antioxidant using DPPH photometric assay

An exact amount (0.5ml) of the methanolic solution of DPPH was added with 10, 20, 30, 40, 50µl of different concentration nanoparticles and 0.48ml of methanol, and allowed to stand at room temperature for 30 minutes. Methanol served as the blank. After 30 minutes, the absorbance was measured at 518nm and converted into percentage radical scavenging activity as follows:

$$\text{Scavenging activity (\%)} = \frac{A_{518}\,[\text{sample}] - A_{518}\,[\text{blank}]}{A_{518}\,[\text{blank}]} \times 100$$

Inhibition of *in vitro* generation of radical scavenging activity

In the present study, the efficiency of the leaves and stems extracts of *C. gigantea (L.) R.Br* in inhibiting

the *in vitro* generation of superoxide, nitric oxide (18) and hydroxyl radical scavenging activity were studied

Antimicrobial activity:

Culture and Maintenance of Bacteria

Gram-positive (*B. subtilis* and *S. aureus*) and Gram-negative (*P. aeruginosa* and *E. coli*) bacteria were used from our laboratory culture collection. The cultured bacteria was transferred into test tubes with nutrient broth (NB) followed by incubation without agitation for 24 h at 37°C. Maintained cultures were used for further assays.

Antibacterial activity- Well Diffusion assay:

Agar well diffusion method (19) was used to study the antibacterial activity of Cg-AgNPs against Gram-positive (*B. subtilis* and *S. aureus*) and Gram-negative bacteria (*P. aeruginosa* and *E. coli*). We maintained bacterial cultures were inoculated uniformly on MHA plates that were prepared by sterile Muller Hinton Agar (MHA) medium. For loading the Cg-AgNPs of leaves and stem at concentration (50µg/ml) the well (6 mm diameter) was constructed on MHA plate with the help of sterile corkborer. Incubation lasted 24 h at 37°C after loading the well. The inhibition zone (mm) was measured around the well. The experiments were repeated in triplicate, including controls.

Minimum inhibitory concentration (MIC) and Minimum bactericidal concentration (MBC) assays (20)

MIC and MBC were determined by a microdilution method, using Luria broth (Hi-media, India) and inoculums of 2.5X 10^5 CFU/ml. In brief, (2.5 X 10^5 CFU/ml) of each bacterial strain was added individually to 1 ml of nutrient broth (NB). Different concentrations of test particles (pure suspension of particles was formed by sonication and it acts as a dissolved solution which accurately reflects the amount of silver available in solution to act on the microorganisms) were added to the test tubes containing the test strains. After 24 h of incubation, the MIC values were obtained by checking the turbidity of the bacterial growth. The MIC value corresponded to the concentration that inhibited 99% of bacterial growth (Dash et al., 2012). The minimum bactericidal concentration (MBC) values of the particles were determined according to the standard method (Dash *et* al., 2012). The MBC values were determined by sub culturing the MIC dilutions onto the sterile Muller Hinton agar plates incubated at 37 C for 24 h. The lowest concentration of the nanoparticles which completely killed the tested bacteria was observed and tabulated as MBC level. The MBC value corresponded to the concentration where 100% of the bacterial growth was arrested, compared to the positive control (no treatment). All assays were performed in the Biosafety cabinet.

Bacterial Killing kinetic assay

Killing kinetic assay (20) of Gram-positive (*B. subtilis* and *S. aureus*) and Gram-negative bacteria (*P. aeruginosa* and *E. coli*).strains was studied against Ag NPs by the method of Guggenbichler et al., (1985). Bacterial growth after treatment (at their respective MBC values) was measured by quantifying cell viability at 0, 2, 4, 8, 12, 18 and 24 h after incubation with Ag NPs. The growth inhibition percentage was obtained with respect to the positive control. Bacterial cell viability was measured spectrophotometrically using Shimadzu UV/vis 1800 spectrophotometer

BGI % = (BC − BT) x 100 / BC

Where BGI = Bacterial Growth Inhibition; BC = Number of Bacterial Colonies.

Antifungal Activity -Well Diffusion Assays:

The sensitivity of *C. albicans* and *A. niger* were evaluated by the well diffusion method on a Mueller-Hinton medium supplemented with 2% glucose and 0.05% methylene blue. In mediums containing Candida sp, wells were made and filled with 80 µg of AgNPs. Discs of amphotericin B 10 µg were used as control. The plates were incubated at 35 °C for 24h, and after this period fungal growth inhibition halos were measured (mm). Each test was conducted three times, according to the protocol of CLSI M44-A2 (22, 23, 24).

Antibiofilm activity

Pseudomonas aeruginosa MTCC 2543 and *Staphylococcus aureus* were collected from MTCC Pune. The microtitre plate technique was followed to analyse the biofilm (30) inhibition of Gram positive (*S. aureus*) and Gram-negative bacteria (*P. aeruginosa*).

Antiangiogenic assay- Chorioallantoic Membrane Assay (CAM)

Fertilized eggs were randomly divided into two groups; the control group and experimental group (treated with concentration of 200 µg mL^{-1} AgNPs) and then incubated at 37°C and 55-65% humidity in the incubation system (Ribatti, 2010). On day eighth of incubation, shells were opened in laminar hood and filter discs (6 mm) were dipped in the extract, dried and placed on the chorioallantoic membrane and incubated at 37°C. On the 12th day of incubation, all the cases were photographed using a research

photo stereomicroscope (Ziess, India).

$$\% \text{ inhibition} = \frac{\text{No .of vessels in untreated - No. of vessels in treated}}{\text{No .of vessels in untreated}} \text{ X } 100$$

Ovicidal and Larvicidal assay:

Collection of eggs and maintenance of larvae:

Mosquito eggs were provided by Indian Council of Medical Research (ICMR) Madurai (Tamil Nadu, India). According to Dinesh et al. (26), the collected eggs were placed in 18 x13 x 4-cm steriled plastic containers filled with 500 mL of water. The eggs hatched and the larvae were fed with a mixture of crushed dog biscuits and yeast at 3:1 ratio. These larvae were used for further studies.

Mosquito ovicidal assay:

Effect of the extracts of silver nanoparticles synthesized using the leaves and stems of *Calotropis gigantea (Linn.) R.Br* on the hatchability of *Anopheles stephensi, Aedes aegypti,* and *Culex quinquefasciatus* eggs were determined and hatching rate was calculated on the basis of non-hatchability of eggs. Five replications were conducted at each extracts concentration (%). Egg hatching rate was monitored for 24h. The assays were developed at 25°C. Of continuous exposure and this was expressed as percent mortality.

Mosquito larvicidal Activity:

Following the standard larvicidal assay by WHO (27), five sets (n = 6 larvae each) of third instar larvae were separated in 50 ml water. Extractof leaves and stems of *Calotropis gigantea (Linn.) R.Br* (50 mg/l), $AgNO_3$ (50 mg/l) and AgNPs of leaves and stem extracts (10 mg/l) were added into the above set up to find out the larvicidal activity. No food as given to the larvae during the assays. The experiments were carried out in three replicates, the control was maintained the distilled water. The larval mortality was evaluated over different time exposure (24 h).The assay was performed by exposing twenty (I, II, III and IV instar) larvae of *Anopheles stephensi, Aedes aegypti, and Culex quinquefasciatus*. The water temperature maintained at 25 ± 1°C. For each test three beakers containing distilled water and test larvae but without sample were used as controls. Observation on mortality and deformities of the larvae was recorded after every 24 hrs. Larvicidal rate was monitored for 24h. The assays were developed at 25°C. Of continuous exposure and this was expressed as percent mortality, the lethal concentration considered at which 50% of the test larvae were killed. The control was set up by mixing 1 ml of acetone with 249 ml of dechlorinated water. The ova and larvae were exposed to dechlorinated water without acetone served as control. The control mortalities were corrected by using Abbott's (1925) formula (28).

$$\text{Mortality} = \frac{\text{(Observed mortality in treatment – Observed mortality in control)}}{\text{100 - Control mortality}} \text{ x } 100$$

$$\% \text{ mortality} = \frac{\text{Number of dead ova/ larvae}}{\text{Number of ova/ larvae introduced}} \text{ x } 100$$

***In vitro* cell viability studies-Cytotoxicity assay - MTT assay:**

Cells were seeded in a 96 well plate. Cells were exposed to the nanoparticles of leaves and stems of *Calotropis gigantea (Linn.) R.Br*. The resulting intracellular purple formazan solubilized the MTT crystals by adding and quantified by spectrophotometric mean and then the supernatants were removed. For solubilization of MTT crystals, 100 µl DMSO was added to the wells. The plates were placed on a shaker for 15 mints for complete solubilization of crystals and then the optical density of each well was determined. The quantity of formazan product was measured by the amount of 545 nm.

Cell proliferation inhibition (%) = (1- OD $_{Sample}$ / OD $_{Control}$) x 100

Viable cells% = (OD of drug-treated sample/ OD of untreated sample) x 100

Statistical analyses

All the experiments were done in three replicates and the results were expressed as Mean ± Standard Deviation (SD).

RESULTS AND DISCUSSION:

Plants are rich sources of natural products used for centuries old to cure various diseases. A retrospection of the healing power of plants and our return to natural remedies is an essential need for all. In the present study, Leaves and stems of *Calotropis gigantea (Linn.) R.Br* were collected in and around Azhagar hills, Madurai district and were authenticated by Dr. S. John Britto S.R in Rapinat Herbarium as "MVS OO14 *Calotropis gigantea (Linn) R. Br"* Trichy, Tamil Nadu, India. The present study was focused to elucidate the influence of *C. gigantea (L.) R. Br* leaves extract-synthesized silver nanoparticles in the cellular and physiological systems. Screened their phytochemicals present in leaves and stems extracts of *C. gigantea (Linn) R. Br* and the silver nanoparticles were successfully

synthesized from $AgNO_3$ through a simple green and natural route using the leaves and stems of *C. gigantea (Linn) R. Br.*

Phytosynthesis of silver nanoparticles

The reduction property of the *C. gigantea (Linn.) R.Br* using silver nitrate solution was studied, by which silver nanoparticles are derived from the plant leaves and stems extract individually. This is due to the phytochemical components present in the leaves and stems extracts, which helps in the reduction of silver ions. The aqueous silver nitrate solution was turned to brown color within 30 min, with the addition of leaves and stems extract. Intensity of brown color increased in direct proportion to the incubation time. It may be due to the excitation of surface Plasmon resonance (SPR) effect and reduction of $AgNO_3$.**Figure 1** shows the reduction of silver nitrate solution by the plant leaf extract and the formation of silver nanoparticles. **Figure 2** shows the complete reaction mixture after 24 hours incubation in a dark room.

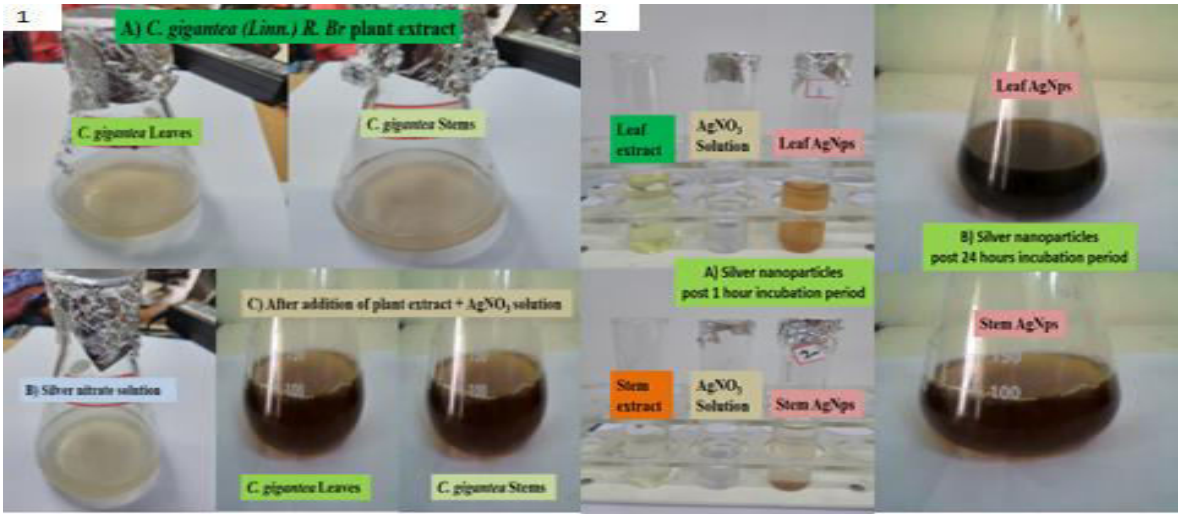

Figure 1 shows the phytosynthesis of silver nanoparticles (A) *C. gigantea (Linn.) R.Br*plant extract (B) silver nitrate and (C) after addition, Figure 2 shows the Silver nanoparticles post 1 hour (A) and 24 hours (B) incubation period.

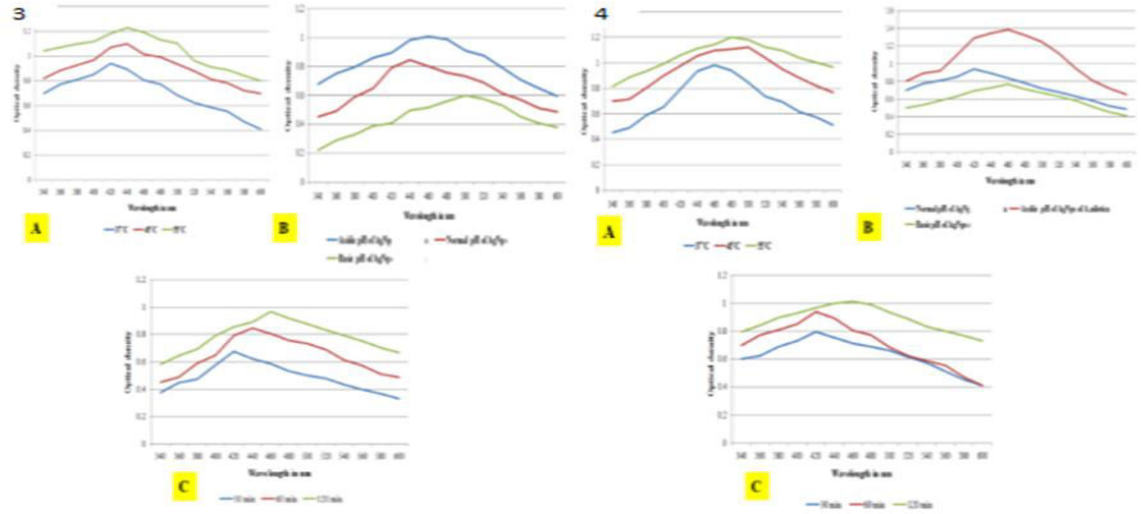

Figure 3 shows the optimization of *C.gigantea* leaf extract-Effect of A) temperature, B) pH C) time of incubation on the formation of silver nanoparticles.

Figure 4 shows the optimization of *C.gigantea* stem extract- Effect of A) temperature, B) pH C) time of incubation on the formation of silver nanoparticles.

Optimization of different parameters

The silver nanoparticles synthesized by using *C. gigantea (L.) R.Br* leaf and stem (**Figure 3** for leaf and **Figure 4** for stem) extract were optimized by various parameters such as different concentrations of silver nitrate, temperature, pH, time of incubation and ratio of plant extract to silver nitrate solution. It is evident from the different concentration in that 1 mM conc. maximally favors the formation of silver nanoparticles. The size is reduced initially due to the reduction in aggregation of the growing nanoparticles. **Figure 3** for leaf and **Figure 4** for stem shows that a slightly alkaline condition enhances and accelerates the formation of silver nanoparticles but the acidic condition deteriorates the formation of silver nanoparticles. Large nanoparticles were formed at lower pH (pH 5), whereas small and highly dispersed nanoparticles were formed at high pH (pH 8). At slightly alkaline pH, the normal size of the nanoparticles was formed in **Figure 3B** and **Figure 4B**shows that duration of reaction increases, more silver nanoparticles are formed. Due to the instability of the silver nanoparticles formed, an optimum duration is required, as silver nanoparticles agglomeration after the optimum duration resulting in larger particle sizes. The optimum time **(Figure 3C**and **Figure 4C)** required for the completion of reaction from our study was 30 min. As the temperature increased, the rate **(Figure 3A**and **Figure 4A)** of silver nanoparticles formation also increased but it started decreasing as the temperature exceedind beyond the 70^0C.Ratio of silver nitrate solution (1 mM) and the leaves Aextract was altered to investigate the optimum composition to maximize the yield of silver nanoparticles. Enough leaf extract must be added to reduce the silver nitrate present in solution. It was found that the optimum ratio for the reaction is 1:9 based on the number of trials and the optimum yield.

The overall optomized reaction condtion was: temperature-60^0C, time- 24 hours, concentration of silver nitrate- 1 mM, pH- 8.0 (slightly alkaline) and the ratio of silver nitrate solution and *C. gigantea (L.) R.Br* leaf / stem extract was 1:9**.**

Characterization of synthesized silver nanoparticles

UV-Visible spectrophotometer

An immediate reduction of silver ions within 10 minutes may be because of the presence of water soluble phytochemicals likes alkaloids, phenolic, flavonoids, sugars and saponins in *C. gigantea (L.) R.Br* leaf and stem extract. It was observed the reduction of silver ions occur rapidly and more than 90% reduction of silver ions is complete within 8 hours and 20 hours respectively, after adding the aqueous plant extract to the metal ions solution. **Figure5**shows the characteristic absorption peak at 418 nm in UV-visible spectrum confirmed forming silver nanoparticles. The nanoparticles showed an absorption peak around 420 nm after 8 h of reaction, which is a characteristic surface plasmon band of silver nano particles possibly because of exciting longitudinal plasmon vibrations in silver nano particles in the solution.

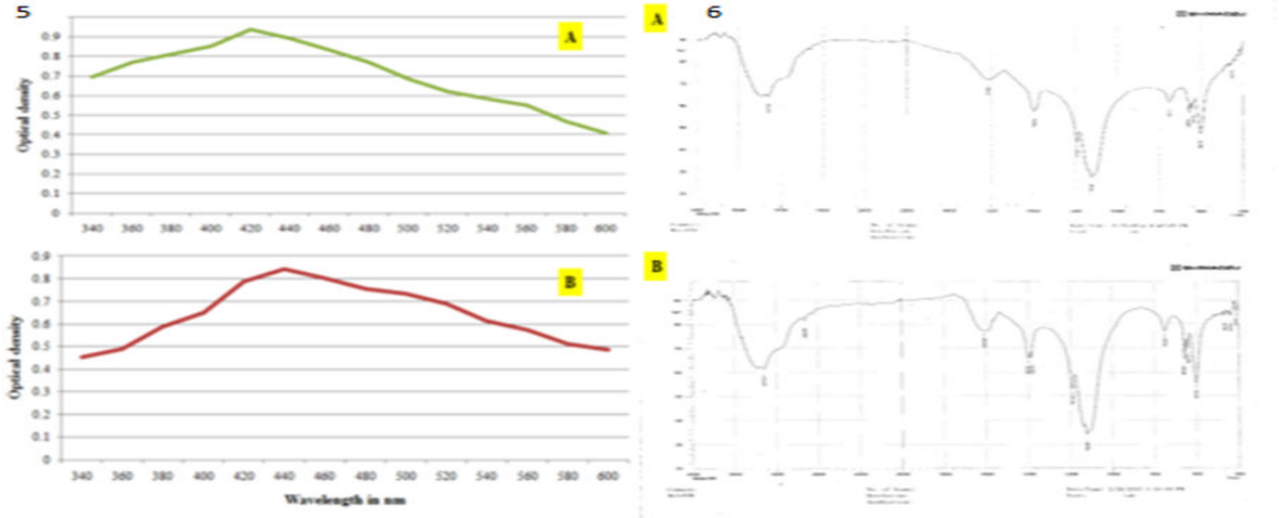

Figure 5 shows the UV Spectra of silver nanoparticles synthesised using *C.gigantea* A) leaf and B) stem extracts, Figure 6 shows the FT-IR Spectra of silver nanoparticles synthesised using C.giganteaA) leaf and B) stem extract.

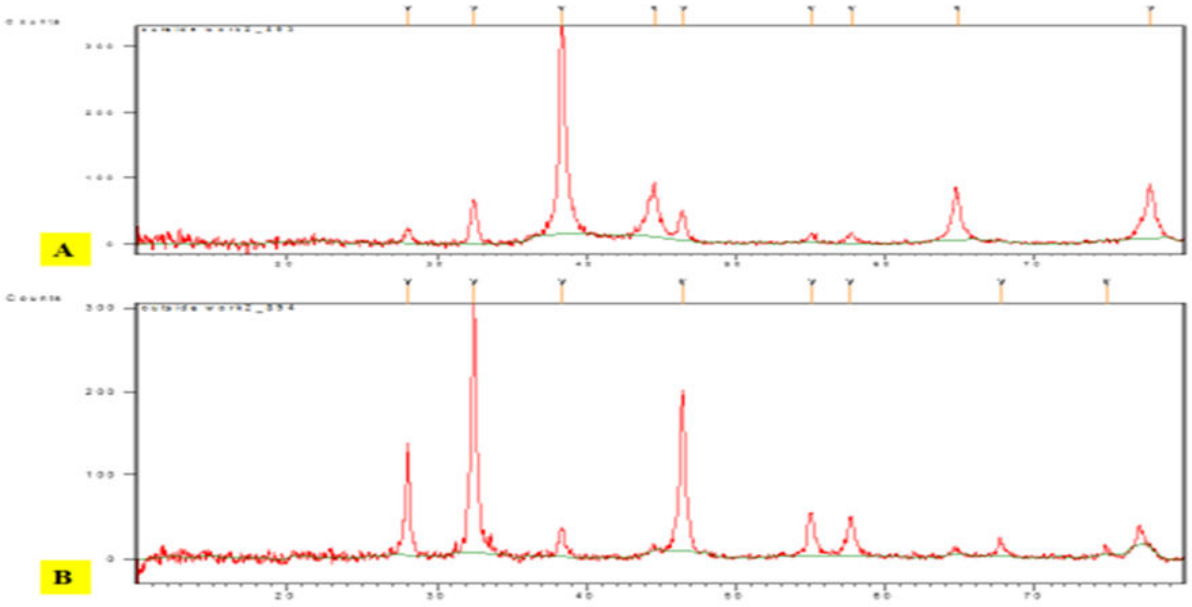

Figure 7 shows the XRD analysis of *C.gigantea* A) leaf and B) stem extract.

Fourier Transform – Infra Red spectral analysis

FTIR measurement was carried out to identify the potential biomolecules and functional groups in the *C. gigantea (L.) R. Br* aqueous plant extract responsible for reducing the silver ions. Different functional groups and structural features in the molecule absorb at characteristics frequencies. The frequency and intensity of absorption are the indication of the band structures and structural geometry of the molecule.**Figure 6** shows the FT-IR spectrum of *C. gigantea (L.) R. Br*. A strong sharp peak was obtained. FTIR measurements carried out to identify the possible biomolecules responsible for the capping and efficient stabilization of the silver nanoparticles synthesized by the plant extracts. (Figure 6 a and b) show the leaf extract of C.gigantea and stem extract of C.gigantea respectively Absorbance bands AgNps of leaf extract of C.gigantea were observed at 3317.34 Cm-1 assigned to O-H (s) stretch, 3317.34 Cm-1 assigned to O-H (s) stretch, 1614.31 Cm-1 assigned to C=C aromatic stretch, 1394.44 Cm-1 assigned to C-H alkenes stretch, 1191.93Cm-1 assigned to C-N amines stretch, 752.19 Cm-1 and 655.75 Cm-1 assigned to C-H alkenes stretch. In figure 6 b shows the absorbance bands of AgNps of stem extract of C.gigantea were observed at 3317.34 Cm-1 assigned to O-H (s) stretch, 2933.88 Cm-1 assigned to C-H (s) stretch, 1606.59 Cm-1 assigned to C=C aromatic stretch, 1394.44 Cm-1 assigned to C-H alkenes stretch, 1191.93 Cm-1 assigned to C-N amines stretch,1122.49 Cm-1 assigned to C-N amines stretch 752.19 Cm-1 and 655.75 Cm-1 assigned to C-H alkenes stretch. Thus, many of the potential biomolecules present in the leaf extract and metal ions present in the silver nitrate solution has been reduced to form silver nanoparticles.

XRD analysis of green silver nanoparticles

The X- ray structural diffraction pattern of the green synthesized silver nanoparticles produced using the leaf extract were further proved and confirmed by the characteristic peaks observed in the XRD image of silver (**Figure 7**). The average grain size of the silver nanoparticles formed in the bio reduction were determined using scherr's formula, $d= (0.9\ \lambda \times 180^0) / \beta \cos\theta\pi$ and estimated as 38.5 nm.

Scanning Electron Microscopic analysis of synthesized silver nanoparticles

The SEM analyses of bio reduced silver nano particles confirmed the morphology and size of the metal particles is in the nano-range and are roughly square in shape. The size of silver nano particles are in the range of 40 and 70 nm after 24 h and the representative SEM images are shown in **Figure 8 a and b.** The characterization of silver nanoparticles was done by using Scanning Electron Microscope (SEM). SEM image of the silver nanoparticle synthesized in which indicates well dispersed particles that are more or less spherical.

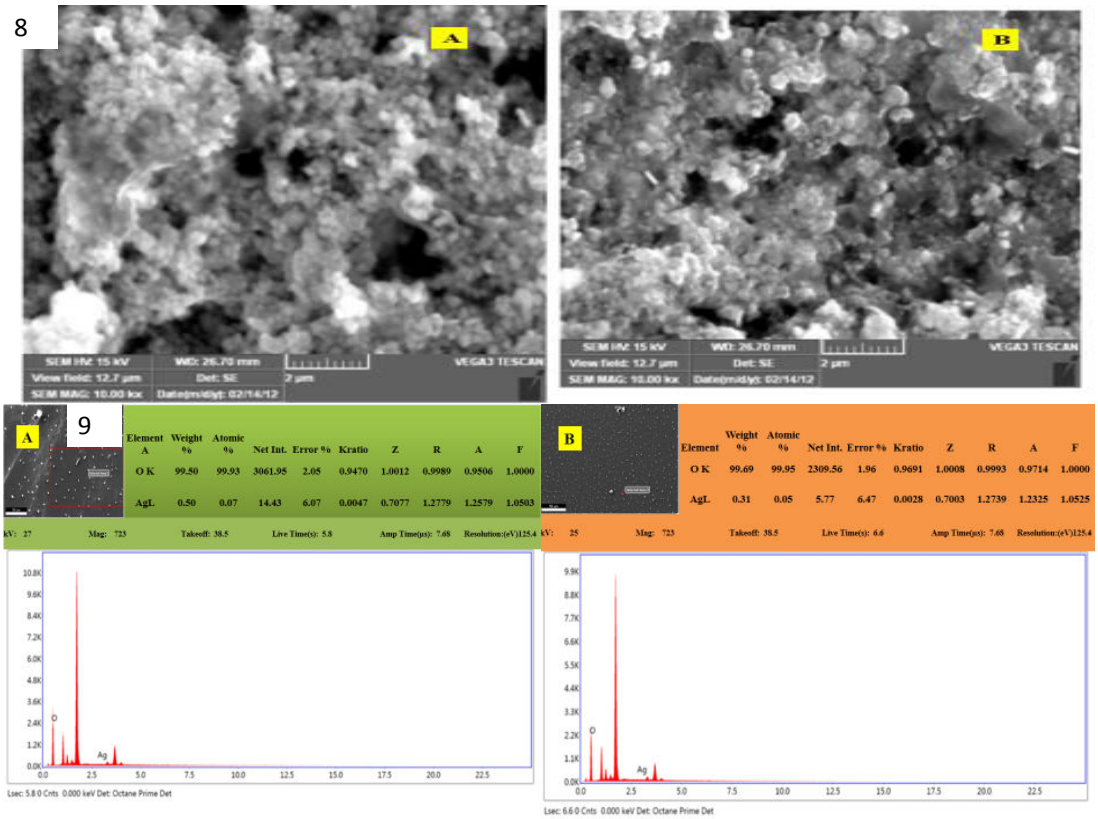

Figure 8 shows the SEM micrograph of Silver nanoparticles synthesized by using the A) leaf extract of *C. gigantea* and B) stem extract of *C. gigantea*.
Figure 9 shows the EDX analysis of *C.gigantea* A) leaf and B) stem extract.

Energy-Dispersive X-ray analysis of silver nanoparticles

The analysis through energy dispersive X-ray spectrophotometers confirmed the presence of elemental silver signal of the silver nanoparticles as shown in **Figure 9a and b**. The vertical axis displays the number of x-ray counts while the horizontal axis displays energy in KeV. The identification lines for the major emission energies for silver are displayed and corresponding with peaks in the spectrum, thus indicating that silver is main elemental component present in the synthesized metal nanoparticles.

Silver nanoparticles (AgNPs) are a new kind of material with several applications, such as sensors, catalysts, anticancer agents and antimicrobial agents. AgNPs have exhibited activity against bacteria, fungi and viruses (29). However, synthesis of AgNPs produces toxic waste, such as ammonia (30), which can affect human health and the environment (31). The green synthesis of AgNPs has used various routes: plants, microorganisms and non-toxic substances (32, 33, 34).

***In vitro* Antioxidant Assay**

The results showed that the radical-scavenging ability of green synthesized silver nanoparticles of *Calotropis gigantea (Linn.) R.Br* was estimated by comparing the percentage inhibition of formation of DPPH, SO, OH and NO radicals with that of ascorbic acid. The DPPH scavenging activity (**Figure 12),** super oxide scavenging assay (**Figure 13),** hydroxyl radical scavenging activity (**Figure 14),** and nitric oxide radical scavenging activity (**Figure 15**) of silver nanoparticles increased with increasing in concentration. In this present study, DPPH, SO, OH and NOradical scavenging effect of silver nanoparticles shows activity in dose dependent manner. The obtained results are compared with standard ascorbic acid.

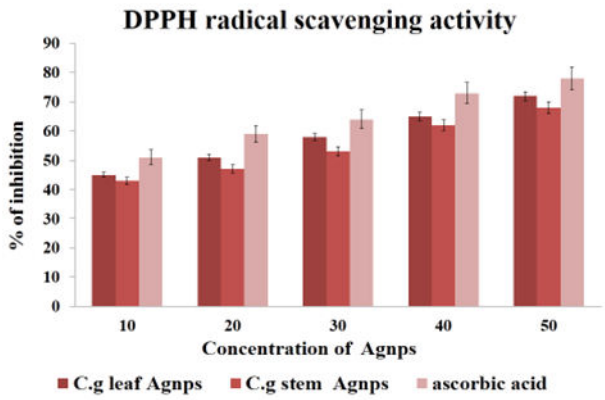

Figure 12: Antioxidant assay by DPPH radical scavenging activity of silver nanoparticles

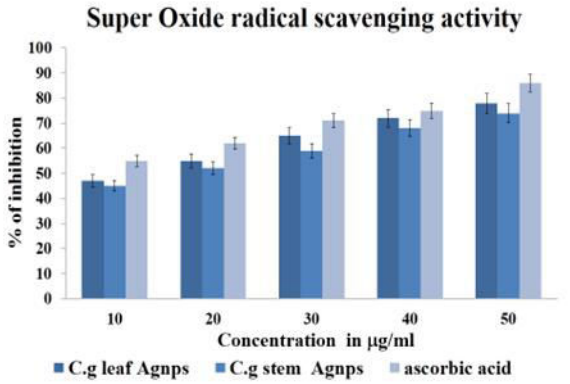

Figure 13: Antioxidant assay by Superoxide radical scavenging activity of silver nanoparticles

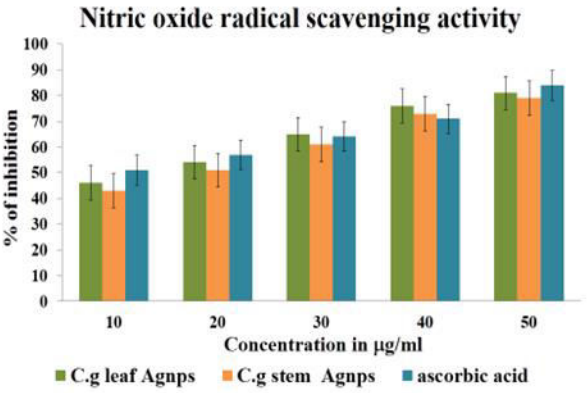

Figure 15: Antioxidant assay by nitric oxide radical scavenging activity of silver nanoparticles

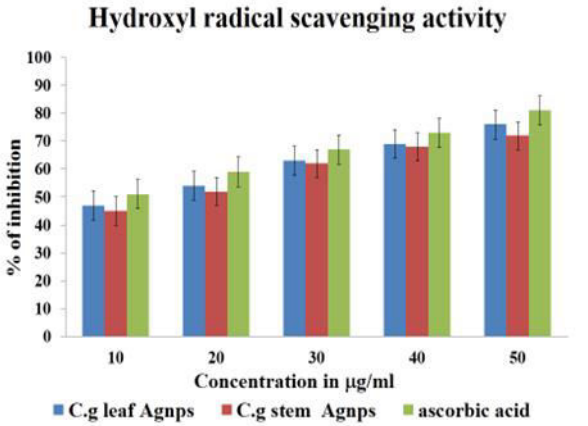

Figure 14: Antioxidant assay by Hydroxyl radical scavenging activity of silver nanoparticles

Antibacterial activity of Ag NPs

The antimicrobial activity of synthesized Ag nanoparticles against four different bacterial pathogens such as *E.coli, P.aerogenosa,* (gram negative bacteria) and *B.subtilis, S.aureus* (gram positive bacteria). Bacterial membrane proteins and DNA makes preferential sites for silver nanoparticles interaction as they possess sulphur and phosphorus compounds and silver have higher affinity to react with these compounds. A clear zone of inhibition was seen around the disc containing the synthesized silver nanoparticle (50 µg/ml) and Standard antibiotic disc (50µg/ml) Amphicillin. These results are shown in **Figure 10**.

In the present study, the antibacterial activity of *Calotropis gigantea (Linn.) R.Br* leaf and stem Cg-AgNPs was tested againstgram-negative (*E. coli, P.aerogenosa)* and gram-positive (*B.subtilis, S. aureus)* bacteria. The*Calotropis gigantea (Linn.) R.Br* leaves and stem extract showed zone of inhibition against *E. coli, P. aeruginosa, B.subtilis* and *S. aureus* when tested at 50 µg/ml, the growth inhibition efficacy was dose-dependent (P\0.01). Testing 50 µg/ml of AgNO3, the zone of inhibition against *E. coli, P.aerogenosa, B.subtilis* and *S.aureus*were 31, 27, 29 and 26mm for leaves and 39, 24, 23 and 23 mm for stems respectively. This result shows that it is well known that Gram-negative bacteria do not have an outer membrane, thus antibacterial substances can easily penetrate the inner membrane.

Minimum inhibitory concentration (MIC) and Minimum bactericidal concentration (MBC) assays

Antimicrobial activity of biosynthesized AgNPs against both gram-negative *E. coli, P.aerogenosa a*and gram-positive *B.subtilis, S. aureus* microorganisms at different concentrations showed that they revealed a strong dose-dependent antimicrobial activity against both of the test microorganisms (**Table 2**). The antimicrobial activity (MIC and MBC) of plant extract was absent until 100µg/ ml against both of the bacterial strains. It was

found that, as the concentration of biosynthesized nanoparticles was increased, microbial growth decreases in both the cases. Biosynthesized Ag NPs were observed to exhibit more antimicrobial activity on gram-negative microorganism than gram positive ones.

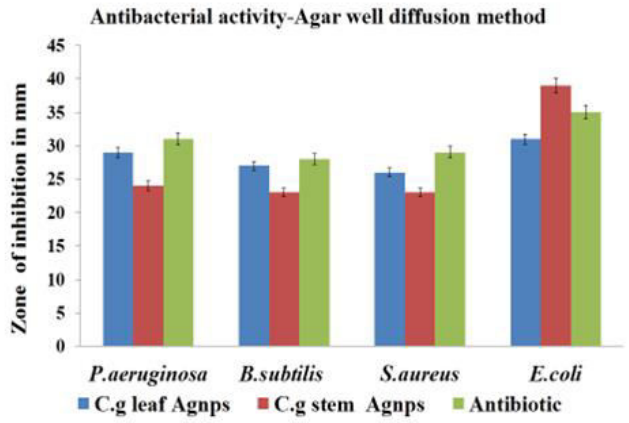

Figure 10 shows the Anti-bacterial zone of inhibition of the synthesized silver nanoparticles of different bacterial pathogens.

Silver nanoparticles	pathogenic microorganisms							
	Pseudomonas aeruginosa		*Staphylococcus aureus*		*Escherichia coli*		*Streptococcus viridians*	
	MIC	MBC	MIC	MBC	MIC	MBC	MIC	MBC
C. g leaf	30	30	40	40	50	50	50	50
C. g stem	30	30	40	40	50	50	50	50

Table 2 shows the Anti-bacterial zone of inhibition of the synthesized silver nanoparticles of different bacterial pathogens.

Table 3 (a): Bacterial killing kinetics for silver nanoparticles of C. g leaf

Silver nanoparticles (µg/ml)	*Staphylococcus aureus*	*Bacillus subtilis*	*Escherichia coli*	*Pseudomonas aeruginosa*
0	260	276	240	290
10	205 (21.1%)	200(27.5%)	180(25%)	220 (24.1%)
20	169 (35%)	174(36.9%)	164(31.6%)	196 (32.4%)
30	136 (47.6%)	150(45.6%)	148(38.3%)	157 (45.8%)
40	108 (58.4%)	120(56.5%)	124(48.3%)	128 (55.8%)
50	58 (77.6%)	48(82.6%)	62(74.1%)	95 (67.2%)

Table 3 (b): Correlation coefficient of silver nanoparticles of C. g leaf against pathogenic microorganisms

Correlation	'r' value
Silver nanoparticles Vs *Staphylococcus aureus*	-0.9946
Silver nanoparticles Vs *Bacillus subtilis*	-0.9772
Silver nanoparticles Vs *Escherichia coli*	-0.9685
Silver nanoparticles Vs *Pseudomonas aeruginosa*	-0.9869

Table 3a & 3b shows the bactericidal effects of leaf Ag NPs on the different bacteria.

Table 4 (a): Bacterial killing kinetics for silver nanoparticles of C. g stem

Silver nanoparticles (µg/ml)	*Staphylococcus aureus*	*Bacillus subtilis*	*Escherichia coli*	*Pseudomonas aeruginosa*
0	274	264	280	285
10	246(10.2%)	225(14.7%)	240(14.2%)	250(12.2%)
20	213(22.2%)	186(29.5%)	190(32.1%)	202(29.1%)
30	173(36.8%)	151(42.8%)	176(37.1%)	168(41.0%)
40	135(50.7%)	117(55.6%)	125(55.3%)	136(52.2%)
50	85(81.7%)	76(71.2%)	87(68.9%)	98(65.6%)

Table 4 (b): Correlation coefficient of silver nanoparticles of C. g stem against pathogenic microorganisms

Correlation	'r' value
Silver nanoparticles Vs *Staphylococcus aureus*	-0.9950
Silver nanoparticles Vs *Bacillus subtilis*	-0.9996
Silver nanoparticles Vs *Escherichia coli*	-0.9941
Silver nanoparticles Vs *Pseudomonas aeruginosa*	-0.9984

Table 4a & 4b shows the bactericidal effects of stem Ag NPs on the different bacteria.

Bacterial killing kinetics

The killing kinetic assay was used to analyze post-treatment bacterial viability and to define the minimum time necessary to reach an inhibitory or bactericidal effect, since no significant difference was found between the bactericidal effects of AgNPs on the different bacteria. The time–kill curve of Ag NPs against *E. coli, P. aeruginosa a*and gram-positive *B.subtilis, S. aureus* strains is presented in **Table 3a & 3b** for leaf and **Table 4a & 4b** for stem. Bactericidal activity was gradually increased to 8 h exposure of the bacteria against Ag NPs at their respective MBC concentrations for both the strains and entire bacteria were killed within this period. Ag NPs showed a time-dependent and rapid bactericidal activity against the test *E. coli, P. aeruginosa B.subtilis* and *S. aureus* strains, and leads bacteria to early stationary phase, as shown in time–kill curves. In our study, silver nanoparticles were effective in inhibiting bacterial growth in a dose and time dependent manner.

The growth curves of bacteria exposed to AgNPs indicated that it could inhibit the growth and reproduction of both the bacteria. In the present study, after 8 h of nanoparticles treatment, the bacterial cells were killed successfully.

Antifungal activity of Ag NPs

In the present study, showed that high activity against *C. albicans* and *A. niger,* a similar activity observed by the antifungal amphotericin B, and may represent an alternative for treating fungal infections. The AgNPs exhibited high antimicrobial activity, and this property can be very useful, especially against microorganisms resistant to conventional antimicrobials (35).

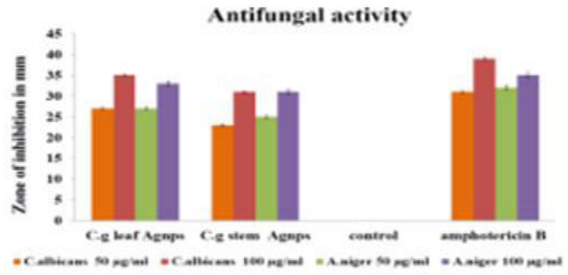

Figure 11 shows the Anti-fungal zone of inhibition of the synthesized silver nanoparticles of different fungal pathogens.

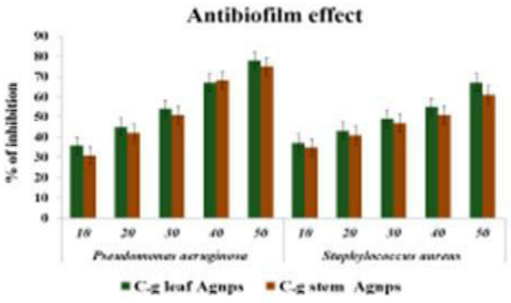

Figure 16: shows the Anti-Biofilm activity of silver nanoparticles

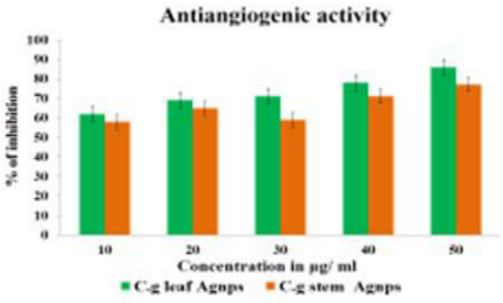

Figure 18: shows the Antiangiogenesis activity of silver nanoparticles

Anti-Biofilm Activity

The increased usage of antibiotics accumulates in the infected animals could also be dangerous to consumers. Here the biofilm inhibitory effects of *Calotropis gigantea (Linn.) R.Br* leaves and stems synthesized Cg-AgNPs against *P.aerogenosa,* (gram negative bacteria) and *S.aureus* (gram positive bacteria) were studied by colorimetric method with crystal violet staining. A perceptible inhibition in the biofilm formation of Gram-positive and Gram-negative bacteria was observed post treatment with Cg-AgNPs at 50 µg/ml under the light microscopic study (**Figure 16**).

Antiangiogenesis activity

Angiogenesis, which is required for physiological events, plays a crucial role in several pathological conditions, such as tumor growth and metastasis. Angiogenesis, which is the formation of new blood vessels from pre-existing ones, is regulated by the balance of many stimulating and inhibiting factors (Otrock *et al*., 2011). The chorioallantoic membrane

(CAM) assay has been proved as a reliable *in vivo* model to study angiogenesis and many inhibitors and stimulators of angiogenesis have been examined by this common method (Ribatti, 2010).

The AgNPs of *C. gigantea (L.) R.Br* leaves and stems extract showed (**Figure18**). Significant antiangiogenic effect in CAM assay. The mechanism of action of AgNPs in preventing the angiogenesis is not known. The AgNPs may hamper the blood vessel formation either by up regulating the inhibitors or down regulation of the stimulators. Further studies of AgNPs at molecular level may help in finding out the mechanism by which the AgNPs act on angiogenesis process.

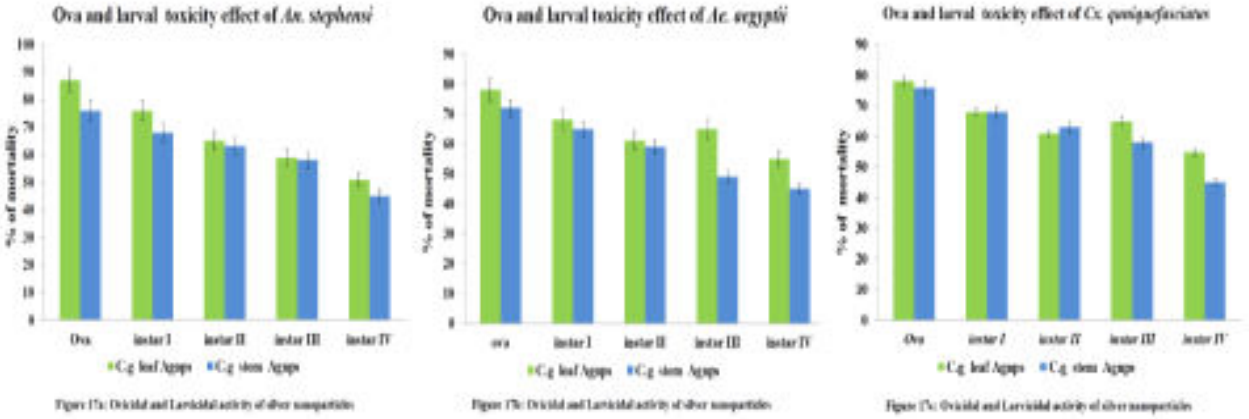

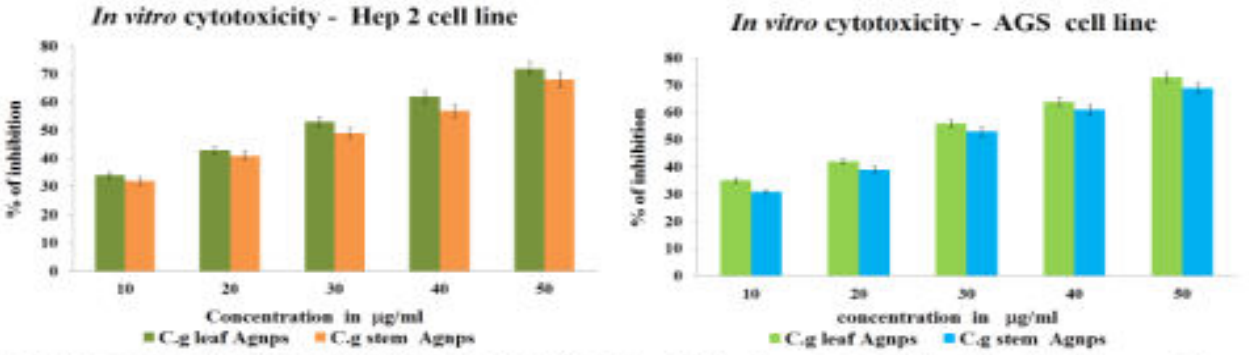

Figure 19 a shows the percentage of inhibition of the synthesized silver nanoparticles on Hep2 cell lines.

Figure 19 b shows the percentage of inhibition of the synthesized silver nanoparticles on AGS cell lines.

Mosquitocidal activity

Recent years green synthesized silver nanoparticles gained much attention due to its high larvicidal potency and less toxic to the environment. Patil et al (37) reported that, the LC_{50} values for second and fourth larval instars of *A. aegypti* after 24 h exposure of synthesized AgNPs using *Plumeriarubra* latex were 1.49, 1.82 ppm, respectively. The potent larvicidal activity noticed in DdAgNPs against dengue vector A. aegypti suggested that it could be used as a possible bio-insecticide in mosquito control programs (38).

Several green approaches have been employed to obtain a reliable and eco-friendly biosynthesis of nanoparticles, which is advantageous over chemical and physical methods. In the present study, *C. gigantea (L.) R.Br* leaves and stems Cg-AgNPs showed ovicidal and larvicidal activity against *Anopheles stephensi* (**Figure17a**), *Aedes aegypti* (**Figure17a**) and *Culex quinquefasciatus* (**Figure17b**). *C. gigantea (Linn.) R.Br* showed 100% mortality of ova and larval I- IV stages of *An. Stephensi*, *A. aegypti* and *C. quinquefasciatus* at 50 mg/l after 48 h. *C. gigantea (L.) R.Br* leaves and stems, AgNO3, Cg-AgNPs showed potent ovicidal and larvicidal activity against *An. Stephensi*, *A. aegypti* and *C. quinquefasciatus*. *C. gigantea (Linn.) R.Br* leaves and stems showed significant lethal concentration against *An. Stephensi*, *A. aegypti* and *C. quinquefasciatus* and the LC_{50} and LC_{90}values were recorded (**Table 5a & 5b**).

***In vitro* cell viability MTT assay**

The activity of silver nanoparticles against Hep2 cells and AGS cells shows in **Figure 19a**and **Figure 19b** which is considered as positive control of Hep2 cells

and AGS cells are shown in purple colour. After we added different concentration of silver nanoparticle in inhibits the Hep2 cells and AGS cells proliferations that are indicated in the Graphical representation. At concentrations higher than 8000ng /ml, they became necrotic and detached from the culture dishes. The dramatic changes induced by silver nanoparticles at concentrations of 100 ng/ml and above.

MTT assay was performed to determine the cytotoxic property of synthesized silver nanoparticles against Hep2 and AGS cell lines. The exposure time of silver nanoparticles in the experiment was 24 hours. The silver nanoparticles were reduced viability of the Hep2 and AGS cells in a dose dependent manner as shown in Figure 19a & 19b. The result obtained shown the IC_{50} at 47.5µg/ml.

Very recently green silver nanoparticles have been synthesized using various natural products like green tea *Camellia sinensis* (39), Neem *Azadirachta indica* (40), leaf broth natural rubber (41), starch (42), *Aloe vera* plant extract (43), lemon grass leaves extract (44, 12), leguminous shrub (*Sesbania drummondii*) (45) etc. Further research is needed to understand the fate of nanoparticles in the aquatic environment. Generally, Ag Inhibits the flow of sodium ions (Na?), by blocking the action of enzymes, Na, K and ATPase, causing a disturbance in ion regulation of aquatic organisms, therefore the toxicity of Ag released by nano-Ag in water should be also considered.

CONCLUSION:

A green synthesis of stable silver nanoparticles using *Calotropis gigantea (Linn.) R.Br* leaves and stems extracts were reported in this study. Synthesis was found to be resourceful in terms of reaction time as well as stability of the prepared nanoparticles which prohibit external stabilizers. It confirms to be an eco-green method for the synthesis providing a cost efficient and a proficient way for the synthesis of silver nanoparticles. In conclusion, AgNPs were easily prepared by green synthesis. The present study suggest that the silver nanoparticles have free radical scavenging activity explored for its applications in the prevention of free radical related diseases and also potential of *C. gigantea (Linn.) R. Br*-synthesised AgNPs for the development of novel antimicrobials, antibiofilm, and antiangiogenesis, mosquitocidal, anticancer and for various purposes.

ACKNOWLEDGEMENT:

Authors gratefully acknowledge the Department of Zoology, The Madura College and Madurai Kamaraj University Madurai, ICMR to carry out this work.

REFERENCES:

1. AmalKumar M, Sanjukta M, Sumana S and Sudebi M. Synthesis of eco-friendly silver nanoparticle from plant latex used as an important taxonomic tool for phylogenetic interrelationship. *Advances in Bioresearch*, 2011; 2 (1): 122 – 133.
2. Mariajancyrani J, Chandramohan G, Ravikumar R. Isolation and identification of phytoconstituents from Delonixregia leaves, *Int J Pharm PharmSci,* 2013; 5(4): 671-674.
3. Britto A J D, Gracelin D H S, Kumar P B J R. Qualitative and quantitative analysis of phytochemicals in Marsileaminuta Linn, *Int J Pharma Bio Sci,* 2013; 4(1): 800-805.
4. Espitia P J P, Soares N F F, Coimbra J S R, AndradeN J, Cruz R S. and MedeirosE A A. Zinc Oxide Nanoparticles: Synthesis, Antimicrobial Activity and Food Packaging Applications, *Food Bioprocess Technol,* 2012; 5: 1447-1464.
5. JonesN, RayB, RanjitK T, Manna A C. Antibacterial activity of ZnO nanoparticle suspensions on a broad spectrum of microorganisms, FEMS *MicrobiolLett,* 2008; 279: 71-76.
6. Namrata S, Piush G, Atul V P, Dr Pathak A K. *Calotropis gigantea*: a review on its phytochemical & pharmacological profile, *International Journal of Pharmacognosy,*2014; 1(1): 1-8.
7. Trease G E, Evans W E. Text book of pharmacognosy, Bacillieretinal Ltd., London, 1989; 13: 7-75.
8. Harborne J B, Phytochemical methods, A Guide to Modern Techniques of Plant Analysis, Chapman & Hall, London, 2005, 2: 85, 86, 126, 196.
9. Sofowra A. Medicinal Plants And traditional Medicine in Africa. Spectrum Books Ltd, Ibadan, Nigeria, 1993; 150,191-289.
10. Garima S, Riju B, Kunal K, Ashish R S, Rajendra P S. Biosynthesis of silver nanoparticles using Ocimum sanctum (Tulsi) leaf extract and screening its antimicrobial activity, *J Nano part Res,* 2010; 13(7): 2981-2988.
11. Veerasamy R, Tiah Z X, Subashnini G. Biosynthesis of silver nanoparticles using managosteen leaf extract and evaluation of their antimicrobial activities. *Journal of Saudi Chemical Society,* 2011; 15: 115-120.
12. Shankar S S, Rai A, Ankamwar B, Singh A, Ahmad A, Sastry M. Biological synthesis of triangular gold nanoprisms, *Nat. Mater,* 2004; 3: 482-488.
13. Manopriya M, Karunaiselvi B, Johnpaul JA. Green synthesis of silver nanoparticles from the

leaf extracts of *Euphorbia hirta* and Neriumindicum, *Digest Journal of Nanomaterials and Biostructures*, 2011; 6(2):869 – 877.

14. Savithramma N, LingoRao M, Suvarnalatha D. Evaluation of Antibacterial efficacy of biologically synthesized silver nanoparticles using stem bark of *Boswellia ovalifoliolata Bal.* and *Shorea tumbuggaia Roxb*. *Journal of Biological Science,* 2011; 11(1): 39-45.
15. Prema. Chemical mediated synthesis of silver nanoparticles and its potential antibacterial application, in Progress in Molecular and Environmental Bioengineering, chapter 6, pp. 151–166, InTech, 2010.
17. Mahendran Vanaja, Gnanadhas G, Kanniah P, Shanmugam R, Chelladurai M, Gurusamy A. Phytosynthesis of silver nanoparticles by Cissus quadrangularis: influence of physicochemical factors, *Journal of Nanostructure in Chemistry,* 2013, 3:17.
18. Nabavi SM, Ebrahimzedh MA, Navabi SF.Bahmaneslami MF. In vitro Antioxidant and Free Radical Scavenging Activity of Diospyros lotus and Pyrusboissieriana growing in Iran, *Pharmacognosy magazine*, 2009; 4 (18): 122-126.
19. Balan B, Baskaralingam V, Thenmozhi C, Sekar V, Marimuthu G, Naiyf S A, Shine K, Jamal M K, Giovanni B. Euphorbia rothiana-Fabricated Ag Nanoparticles Showed High Toxicity on Aedes aegypti Larvae and Growth Inhibition on Microbial Pathogens: A Focus on Morphological Changes in Mosquitoes and Antibiofilm Potential Against Bacteria,*JClustSci,* 2017; 1263-4.
20. Dash S K, Chakraborty S P, Mandal D, Roy S. Isolation and characterization of multi drug resistant uropathogenicEscherichia coli from urine sample of urinary tract infected patients,*Int. J. Life Sci. Pharm. Res.*2012; 2: 2250-0480.
21. Guggenbichler J P, Semenitz E, Ko¨ nig P. Kill kinetics and regrowth pattern of bacteria exposed to antibiotic concentrations simulating those observed in vivo, *J. Antimicrob. Chemother,* 1985; 15: 139–146.
22. Clinical and Laboratory Standards Institute. Method for antifungal disk diffusion susceptibility testing of yeasts: approved standard M44-A2. Wayne: Clinical and Laboratory Standards Institute; 2008.
23. Vasconcelos J AA, Menezes EA, Cunha FA, Cunha MCSO, Braz BHL, Capelo L G. Comparação entre microdiluição e disco difusão para o teste de susceptibilidadeaosantifúngicos contra Candida spp,*SeminaCiêncBiolSaúde,* 2012;33:135-42.
24. Mallmann E JJ, Cunha F A, Castro B N M F, Maciel A M, Menezes E A, Fechine P B A. Antifungal activity of silver nanoparticles obtained by green synthesis. *Rev Inst Med Trop Sao Paulo,* 2015; 57(2): 165-7
25. Ribatti D. The chick embryo chorioallantoic membrane as an *in vivo* assay to study antiangiogenesis,*Pharmaceuticals,* 2010; 3: 482-513.
26. Dinesh D, Murugan K, Madhiyazhagan P, Panneerselvam C, Kumar P M, Nicoletti M, Jiang W, Benelli G, Chandramohan B, Suresh U. *Parasitol Res,*2015; 114: 1519–1529.
27. World Health Organization. Report of the WHO Informal Consultation on the Evaluation on the Testing of Insecticides CTD/WHO PES/IC/96, 1996; 1:69.
28. Márcio VR, Glaís de PB, Cléverson D, Teixeira de F, Nádia A P N, Nylane M N A, Petrônio A S de S, Ana Fontenele UC. Latex constituents from *Calotropis procera* (R. Br.) display toxicity upon egg hatching and larvae of *Aedes aegypti* (Linn.).*MemInst Oswaldo Cruz,* Rio de Janeiro, 2006; 101(5): 503-510.
29. Kashyap P L, Kumar S, Srivastava A K, Sharma A K. Myconanotechnology in agriculture: a perspective, *World J Microbiol Biotechnol,* 2013;29:191-207.
30. Panácek A, Kolár M, Vecerová R, PrucekR, Soukupová J, Krystof V. Antifungal activity of silver nanoparticles against Candida spp, *Biomaterials,* 2009;30:6333-40.
31. Shenashen MA, El-Safty SA, Elshehy EA. Synthesis, morphological control, and properties of silver nanoparticles in potential applications, *Part Syst Charact.* 20143231: 293-316.
32. Iravani S. Green synthesis of metal nanoparticles using plants, *Green Chem,* 2011; 13: 2638- 50.
33. Quester K, Avalos-Borja M, Castro-Longoria E. Biosynthesis and microscopic study of metallic nanoparticles, *Micron,* 2013; 54-55: 1-27.
34. Sintubin L, Verstraete W, Boon N. Biologically produced nanosilver: current state and future perspectives, *BiotechnolBioeng,* 2012; 109: 2422-36.
35. Sharma VK, Yngard RA, Lin Y. Silver nanoparticles: green synthesis and their antimicrobial activities, *Adv Colloid Interface Sci*, 2009; 145: 83-96.
36. Otrock, Z K, Hatoum H A ,MusallamK M, AwadaA H, Shamseddine A I. Is VEGF a predictive biomarker to anti-angiogenic therapy? *Crit Rev Oncol Hematol, m* 2011; 79: 103-111.

37. Patil C D, Patil S V, Borase H P, Salunke B K, Salunkhe R.B. *Parasitol. Res,* 2012; 110(5): 1815–1822.
38. Gopal S, Poosali H G, Dhanasegaran K, Durai P, Devadoss D, Nagaiya R, Balasubramanian R, Arunagirinathan K, Ganesan V S. Green synthesis of silver nanoparticles using Delphinium denudatumroot extract exhibits antibacterial and mosquito larvicidal activities, *Spectrochimica Acta Part A: Molecular and Biomolecular Spectroscopy,* 2014; 61–127: 66.
39. Torresdey J L G, Gomez E, Videa P J, Parsons J G, Troiani.H E, Yacaman M J. Alfalfa sprouts: a natural source for the synthesis of silver nanoparticles, *Langmuir,* 2003; 19: 357- 1361.
40. Nestor A R V, Mendieta V S, Lopez C M A, Espinosa R M G, Lopez M A C, Alatorre J A C. Solvent less synthesis and optical properties of Au and Ag nanoparticles using *Camellia sinensis* extract, *AterLett,*2008;62; 3103-3105.
41. ShivShankar S, Rai A, Ahmad A, Sastry M. Rapid synthesis of Act. Ag, and bimetallic Au core-Ag shell nanoparticles using neem (*Azadirachtaindica)* leaf S, broth, *J. Colloid Interf Sci,* 2004; 275:496-502.
42. AbuBakarjIsmail N H H, Abu Bakar M. Synthesis and characterization of silver nanoparticles in natural rubber, *Mater ChemPhys*, 2004; 104: 276-283.
43. Vigneshwaram N, Nachane R P, Balasubramanya R H, Varadrajan P V. A novel one pot 'green'synthesis of stable silver nonoprticles using soluble starch, *Carbohydrate Res,* 2006; 341: 2012-2018.
44. Chandran S P, Chaudhary M, Pasriocha R, Ahmad A, Sastry M. Synthesis of gold nanotriangles and silver nanoparticles using Aloe vera plant extract, *Biotechnol Prog,* 2004; 22: 577-583.
45. Shankar S S, Rai A, Ahmad A, Sastry M. Controlling the optical properties of lemon grass extract synthesized gold nanotriangles and potential application in infrared-absorbing optical coatings, *Chem Mater,*2005; 17: 566-572.